Study of the thermo-mechanical properties of a lead-stainless steel composite at 298 K and 77 K

F. Aretio-Zárate[1*], M. Chalifour[1], M. Aleksa[1], J. Bremer[1], I. Avilés Santillana[1], B. Ruiz-Palenzuela[1], E. Rodríguez Castro[1]

[1] European Organization for Nuclear Research (CERN), Geneva, Switzerland

[*]E-mail: fernando.aretio.zarate@cern.ch

Abstract. ALLEGRO is a proposed FCC-ee general-purpose detector concept with a noble-liquid electromagnetic calorimeter (ECAL) as one of its central detectors. Noble-liquid calorimetry is a strong option for future particle physics experiments – for both, hadron and lepton colliders. Such an ECAL is composed of a sandwich of 1536 multi-layer read-out electrodes realised as PCBs and the same number of absorbers immersed in a liquified noble gas at cryogenic temperatures. The absorbers are made of metallic composites using lead as core and stainless steel as skin. The different thermal contraction coefficients of these materials as well as the resin used to glue them together, cause residual stresses in the layers. A careful study of this composite is needed to characterise its thermo-mechanical behaviour and to avoid high stresses at operating conditions. Theoretical and numerical studies have been conducted, along with strength and contraction tests, to determine the material's yielding point and its thermal contraction between room temperature and 77 K.

1. Introduction

In the framework of the design of the new detector ALLEGRO, where a noble-liquid calorimeter is one of the central detectors [1], the understanding of the components of this last one is required. In sampling calorimeters [2], one of the essential elements are the absorbers which help reaching the required number of radiation lengths while keeping a compact detector.

In the case of the ALLEGRO ECAL, lead is the main material of the absorbers (Figure 1). Its low stiffness requires external layers to enhance rigidity forming a composite material. The ECAL works at cryogenic temperatures, and different coefficients of thermal expansion (CTE) induce additional stress with large temperature changes in sandwich materials, such as the absorbers, or structures. This effect can cause materials to plastify or even collapse. Therefore, the equivalent CTE and the yielding point of the sandwich plates are analysed and tested.



Figure 1. Layers of the absorber: stainless steel (2x0.05 mm), FR4(2x0.05 mm), lead (1.8 mm)

Following the radiation studies, the composite will have 5 layers: a 1.8 mm lead core, two 0.05 mm external sheets of stainless steel and 0.05 mm of fiberglass (FR4) to glue them together.

Content from this work may be used under the terms of the Creative Commons Attribution 4.0 licence. Any further distribution of this work must maintain attribution to the author(s) and the title of the work, journal citation and DOI.
Published under licence by IOP Publishing Ltd

Analytical and simulation studies to calculate the CTE and the yielding point of the sandwich at room temperature (RT), 298 K, and 77 K are performed. Results are compared with the data of strength and contraction tests. Liquid nitrogen was used for practical reasons.

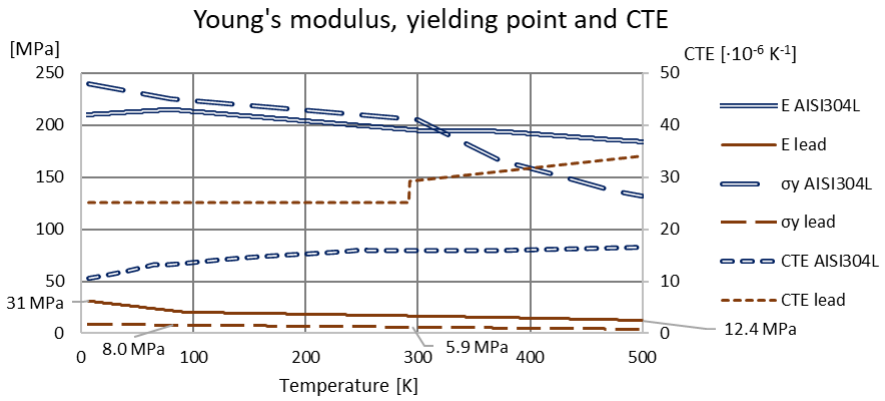


Figure 2. Young's Modulus (E), yielding point (σy) and CTE of lead and AISI304L

Figure 2 presents the material properties of the stainless steel (AISI304L), taken from [3], [4] and [5]. In the case of lead, E and CTE are found in [6], while tests were done at 77 K and RT to determine the yielding points, returning 8.0 MPa and 5.9 MPa respectively.

In the studies, bilinear approximation is used if the material reaches the yielding point. Young's Modulus in plastic region are taken as a percentage of the elastic one, being 0.7% for the stainless steel and 1.5% for the lead. Characteristics of the FR4 are taken from [7], being 24.6 GPa the Young's modulus and $15.5 \cdot 10^{-6}$ K^{-1} the CTE at every stress and temperature.

2. Laminate theory study

The analytical study follows the laminate theory [8] using the material properties described in section 1. Both, RT and cold cases, are studied taking the polymerisation temperature of the fiberglass, 428 K, as the reference point. The study is conducted in two steps: first, the thermal load is applied until 298 K or 77 K, and then the axial force is introduced.

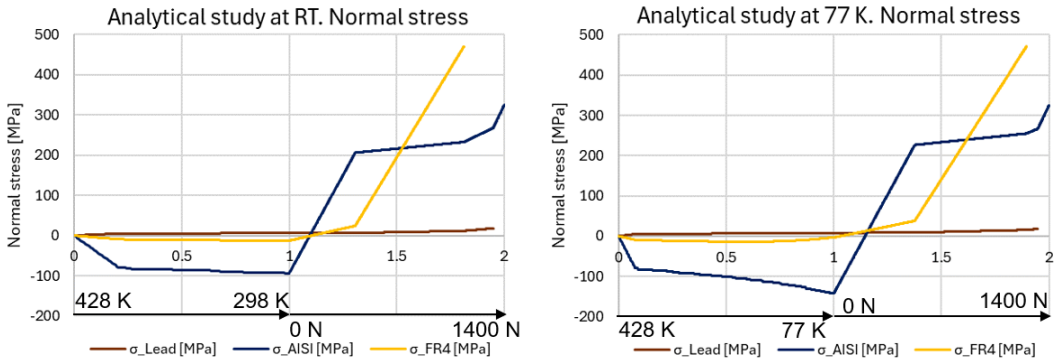


Figure 3. Normal stress of each layer during the cooling process and introduction of the force until the failure occurs.

Each angle change in the stress-strain curves, shown in Figure 3, indicates one of the materials transitioning to non-linear behaviour, except the change in the point 1, where the force

application starts. The lead reaches its yielding point during the cooling while the stainless steel plastifies in the second step. The behaviour of the FR4 is considered linear until failure.

It can be seen how the stainless steel reaches 94 MPa in compression as prestress for the RT condition and 142 MPa in the 77 K one. This will have an impact in the yielding point of the composite, as shown in the graphic of the Figure 4.

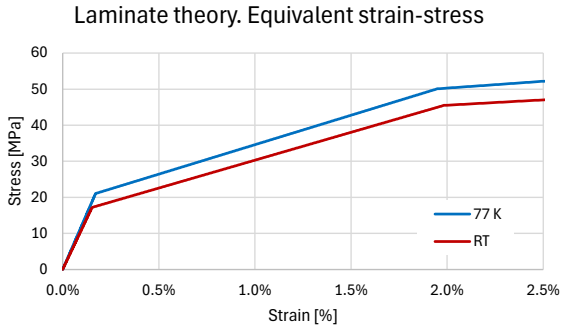


Figure 4. Engineering strain-stress curve of the composite for RT and 77 K.

As indicated by the strain-stress curves of the composite material, the yielding point at RT, according to lamination theory, is 17.2 MPa, whereas at 77 K it reaches 21.1 MPa. The equivalent CTE, dependent on the rigidity of each layer, is also analyzed, being $14.0 \cdot 10^{-6}$ K^{-1} at 77 K.

3. Finite elements model study

Finite Element Analysis (FEA) is employed to study the same scenarios as those examined with laminate theory. Initially, a thermal load is applied, decreasing the temperature from 428 K to either 298 K or 77 K. Subsequently, a tensile load is gradually applied until reaching 1400 N. Material properties from section 1 are used.

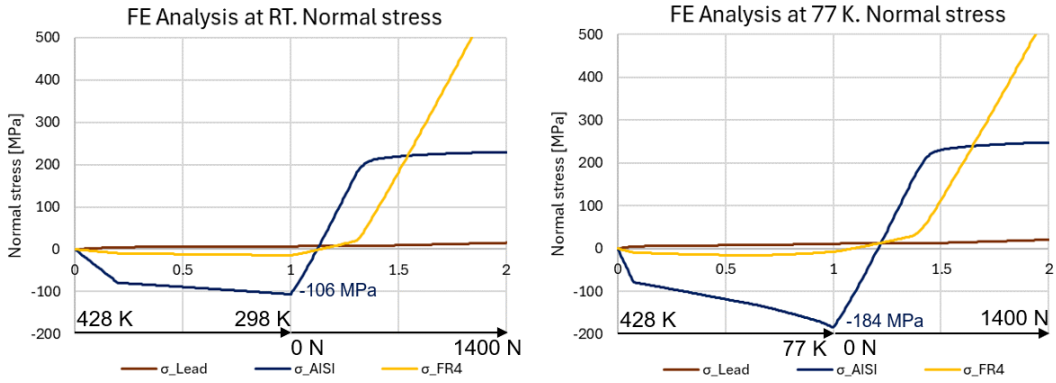


Figure 5. Normal stress of each layer during the cooling down and the application of the force.

The graphs in Figure 5 illustrate the stress response of the materials during the cooling process and under the tension load case. It can be observed that the transitions to non-linear behaviour are curved rather than angular, as not all the elements of the mesh reach the yielding point simultaneously. Lead plastifies during the cooling, causing the compression stress in the stainless steel to increase more gradually. The stainless steel undergoes plastic deformation during the tensile test, moment in which FR4 stress significantly increases.

Stainless steel achieves a compressive prestress of 106 MPa for the room temperature condition and 184 MPa for the 77 K one. This affects the composite's yield point, as depicted in the subsequent graph.

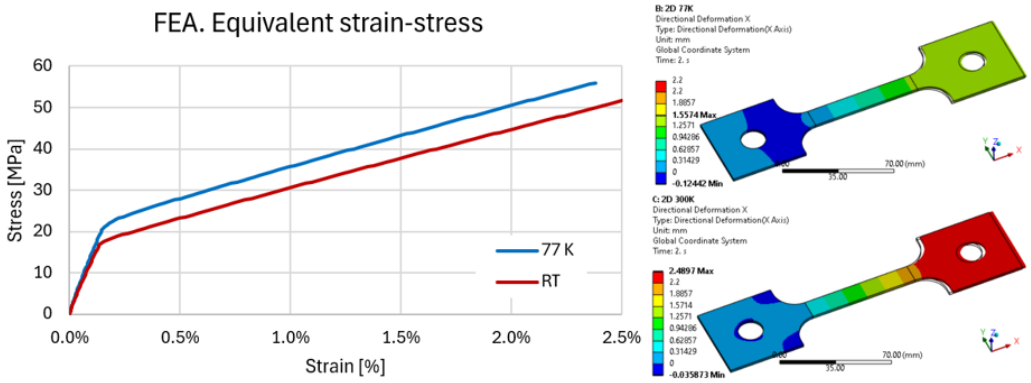


Figure 6. Engineering strain-stress curve of the composite for RT and 77 K. On the left, deformation in X direction is shown for the cold (up) and RT (down) simulations.

The stress-strain curves in Figure 6 indicate that the yield point of the equivalent composite is 17.2 MPa at RT and increases to 20.8 MPa at 77 K. The slope of the elastic region, representing the equivalent Young's Modulus, is slightly larger in the cold study, due to the stiffer properties of the materials. By examining the nodes' displacements in the central region of the geometry, the CTE at 77 K is determined to be $14.5 \cdot 10^{-6}$ K^{-1}.

4. Strength tests

The main objective of the tests is to extract the values of the yielding points ($R_{p0.2}$) of the material, study the sequence of failure, and check the differences between the strain-stress curves at RT and 77 K. Two specimens were tested at RT [9] and five at 77 K [10]. Two of the cold tests were interrupted after the first and the second stress drop to identify the failure mode. Elongation was controlled by the crosshead at 77K and using a video extensometer at RT.



Figure 7. Sandwich specimen [11], set-up, liquid nitrogen bath and a sample after the test at 77 K.

Figure 7 presents photographs from the test, whereas the results are shown in Figure 8. At RT, the material presents the yield point at 16 MPa, whereas under cold conditions, this value increases to 38 MPa. The increase of this value at low temperature was expected considering the properties of lead and stainless steel. Additionally, the stainless steel is compressed by the lead at 77 K due to the different CTE, which moves away the initial prestress from the tension yielding point of this layer, increasing the yielding point of the composite until the 38 MPa.

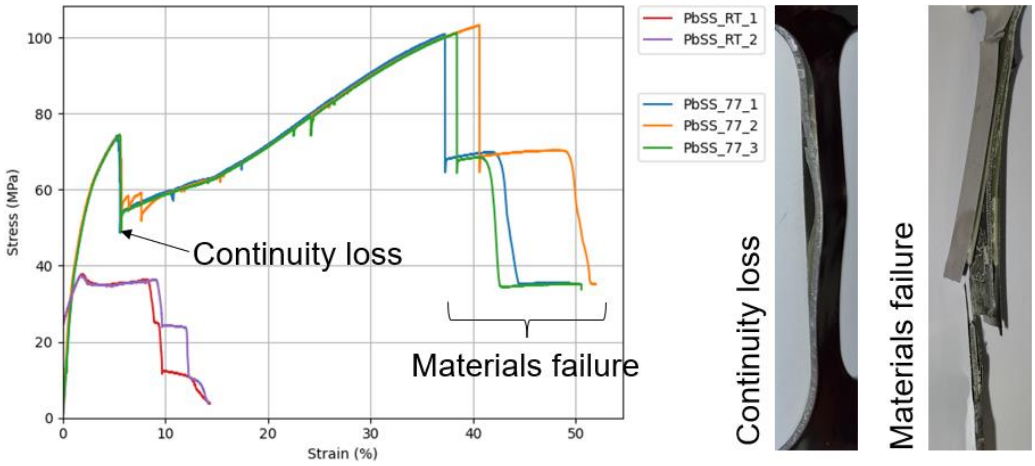
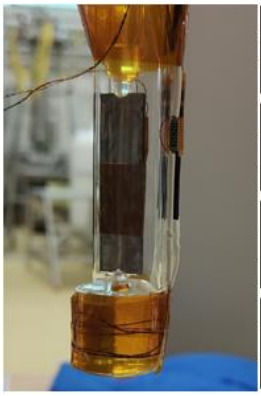


Figure 8. Engineering strain-stress curves. The two on the bottom part are the test at RT. The other three show the complete tests at 77 K. The first photo on the right (*Continuity loss*) has been taken in another test at 77 K that was interrupted to see the phenomenon behind the drop.

Tests at RT and 77 K demonstrate high repeatability, with three distinct segments exhibiting a positive slope. The first segment extends up to the *yielding point*. The second one shows less rigidity, followed by a drop, greater in the 77 K cases. Interrupted test (not shown in the graph) indicate a loss of continuity across the thickness due to degluing and failure of the FR4, causing the loss of compression prestress in the stainless steel. After the drop, the flatter curves suggest the plastification of the stainless steel. Finally, several dips indicate the failure of the materials.

5. Contraction tests

Three samples of the sandwich material are immersed in liquid nitrogen and the contraction is measured to calculate the CTE of the material.



Lead-SS sample 1	Test 1	Test 2	Test 3
Between 273K and 77K	3.31E-03	3.26E-03	3.33E-03
Between RT and 77K	3.48E-03	3.57E-03	3.66E-03

Lead-SS sample 2	Test 1	Test 2	Test 3
Between 273K and 77K	3.55E-03	3.41E-03	3.55E-03
Between RT and 77K	3.65E-03	3.65E-03	3.82E-03

Lead-SS sample 3	Test 1	Test 2	Test 3	Test 4
Between 273K and 77K	2.98E-03	3.10E-03	2.98E-03	3.21E-03
Between RT and 77K	3.13E-03	3.29E-03	3.29E-03	3.31E-03

Lead-SS Average	Average	Std Dev	CTE [1/K]
Between 273K and 77K	3.27E-03	6.32%	1.67E-05
Between RT and 77K	3.49E-03	6.28%	1.56E-05

Figure 9. One of the samples mounted in the set-up for testing, the contraction results ($-\Delta L/L$) and the calculation of the average and the CTE.

The results presented in Figure 9 suggest plastification of the lead during the cold down, as the calculated CTE at 77 K ($15.6 \cdot 10^{-6}$ K^{-1}) is nearer the value of the stainless steel ($13.2 \cdot 10^{-6}$ K^{-1}) than to the value of the lead ($25.1 \cdot 10^{-6}$ K^{-1}). In addition, the machining done in the upper and lower edges of the sample may have induced nonvisible discontinuities in the material. This fact can be responsible for the dispersion of the obtained results.

6. Conclusions

In the context of the design of the electromagnetic calorimeter for the new detector concept ALLEGRO, strength and contraction tests and studies have been performed on a composite material comprising a core of 1.8 mm lead and 0.05 mm stainless steel external layers, using FR4 to glue them together. This material will be used as absorber in the aforementioned calorimeter.

Table 1. Yielding point and CTE obtained in each one of the studies: test, laminate theory and FEA.

	σy at RT [MPa]	σy at 77 K [MPa]	CTE at 77 K [10^{-6} K^{-1}]
Experimental results	16.0	38.0	15.6
Laminate theory	17.2	21.1	14.0
FEA	17.2	20.8	14.5

Table 1 presents the results of the test and the studies performed. From the comparison between the values, it can be stated that the yielding point at room temperature is well approximated by the analytic laminate theory and the FEA. However, they underestimate the yielding point at 77 K and the contribution of the lead in the analysis of the CTE.

This indicates that the stiffness of the plastified lead could be higher than expected at cryogenic temperatures. There are at least two reasons that can explain this divergence. One is that the stiffness of the lead depends on the strain rate. The faster the load is applied, the stiffer the material behaves. Secondly, lead presents dynamic recrystallization at room temperature [12], which brings back some elastic energy to the material, making it stiffer than expected when cooling down from RT to 77 K.

The increased stiffness of the lead can result in greater than anticipated compression prestress on the stainless steel. So, dedicated tests are required to know the exact amount of stress applied to these external layers.

References

[1] Francois, Brieuc, On behalf of the FCC Noble Liquid Calorimetry group (2022) *Noble liquid calorimetry for a future FCC-ee experiment*. https://doi.org/10.1016/j.nima.2022.167035
[2] Aleksa, Martin et al (2021) *Calorimetry at FCC-ee*. https://doi.org/10.1140/epjp/s13360-021-02034-2
[3] Association Française du Froid (2019) *Fascicule de cryogénie et supraconductivité.* (978-2-37620-356-8)
[4] *Stainless steels - Part 2: Technical delivery conditions for sheet/plate and strip of corrosion resisting steels for general purposes*. SN EN 10088-2:2014
[5] *Stainless steels - Part 1: List of stainless steels*. SN EN 10088-1:2024
[6] Hofmann, W (1970) *Lead and lead alloys. Properties and technology.* (DOI 10.1007/978-3-662-28508-4)
[7] *Ansys GRANTA EduPack software*, ANSYS, Inc., Cambridge, UK, YEAR (www.ansys.com/materials)
[8] Nettles, Alan (1994) *Basic mechanics of laminated composite plates*. (NASA-RP-1351)
[9] *Metallic materials - Tensile testing - Part 1: Method of test at room temperature.* SN EN ISO 6892-1:2020
[10] *Metallic materials - Tensile testing - Part 3: Method of test at low temperature.* SN EN ISO 6892-3:2015
[11] Standard Test Methods for Tension Testing of Metallic Materials. ASTM E8/E8M:24
[12] Muramatsu, Mayu (2014) Tensile Testing with Cyclic Strain Holding to Analyze Dynamic Recrystallization of Pure Lead, Advances in Materials Science and Engineering, https://doi.org/10.1155/2014/498674